

# CIRCULAR SITES AT ANGKOR: A RADAR SCATTERING MODEL

Elizabeth H. Moore\*  
and  
Anthony Freeman\*\*

## *Abstract*

The paper describes the use of radar data to detect curvilinear patterns around circular mounds in the Angkor region. The radar data was acquired with equipment of the National Aeronautics and Space Administration and the Jet Propulsion Laboratory. A three-component scattering model is used to assess the presence of water at mound sites. The sensitivity of the radar allows detection of inundated areas covered by low-growing vegetation which are not apparent on optical imagery. The patterns are compared to comparable sites in Northeast Thailand, and used to suggest a similar prehistoric tradition of Khmer water management.

## Introduction

The city of Angkor exploited waters flowing down from the Kulen Hills, a Khmer expertise which grew out of an earlier tradition of water management control in periods of flood and conservation during the dry season. Vestiges of this tradition are detectable on images generated from data acquired by the National Aeronautics and Space Administration/Jet Propulsion Laboratory (NASA/JPL) radar instrument, the Space Imaging Radar version C, Synthetic Aperture Radar carrying the X-Band (SIR-C/X-SAR). The NASA/JPL SIR-C/X-SAR data was obtained when the instrument was carried on space shuttle Endeavour. The instrument was turned on over Angkor on 30 September 1994 during the 15th orbit of Endeavour.

Radar data from three scattering mechanisms form curvilinear patterns which are described here for eleven mound sites in the Angkor region. The sites average 200 metres in diameter and are located at elevations between 11 and 23 metres above sea level. The curvilinear patterns do not necessarily

enclose the mound but are sectors, the locations of which may relate to slope and drainage. It is suggested that these patterns are man-made moats and dikes, remnants of pre-Angkorean (pre-9th century AD) Khmer water management.

Archaeological applications of the NASA/JPL radar have principally been conducted in arid regions. These have detected earlier man-made linear features (e.g. roads at Ubar and along the Silk Road), or climatic changes affecting habitation (such as desiccated subsurface water channels in the Safsaf Egyptian desert). Subsurface detection relies on an absence of ground level moisture and vegetation, allowing shorter and longer wavelengths (X-Band [3 cm], C-Band [6 cm], L-Band [23 cm]) to sense variations in the soil's dielectric constant which may be characteristic of former river beds. At Angkor, stratigraphic interpretation is not completely precluded, as the radar backscatter presents hydrological patterns of different chronological periods. However, the greatest potential is the discrimination of surface variations resulting from the radar's sensitivity to moisture and vegetation.

Initial examination of Angkor using ra-

---

\*School of Oriental and African Studies, University of London, WC1, UK.

\*\*Jet Propulsion Laboratory, Pasadena, USA.

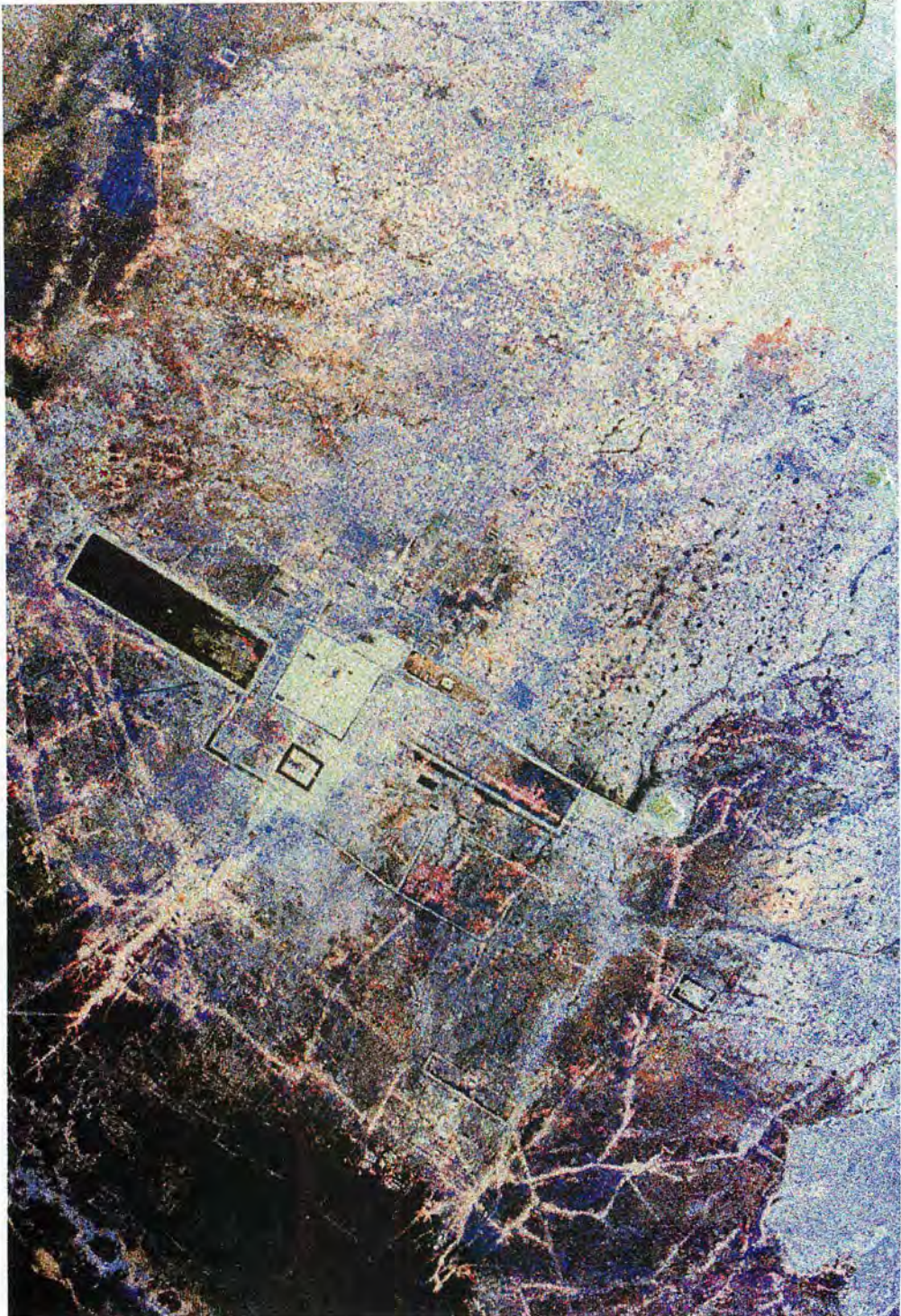


**Figure 1.** Colour composite of the Angkor floodplain. This colour composite is made up of data at L-Band and C-Band. The data in the green channel was sent from the radar antennae polarised horizontally and was returned to the satellite polarised vertically. This is referred to as Lhv. This green band dominates Mt. Kulen, highlighting relief on interior parts. Data courtesy of NASA/JPL.



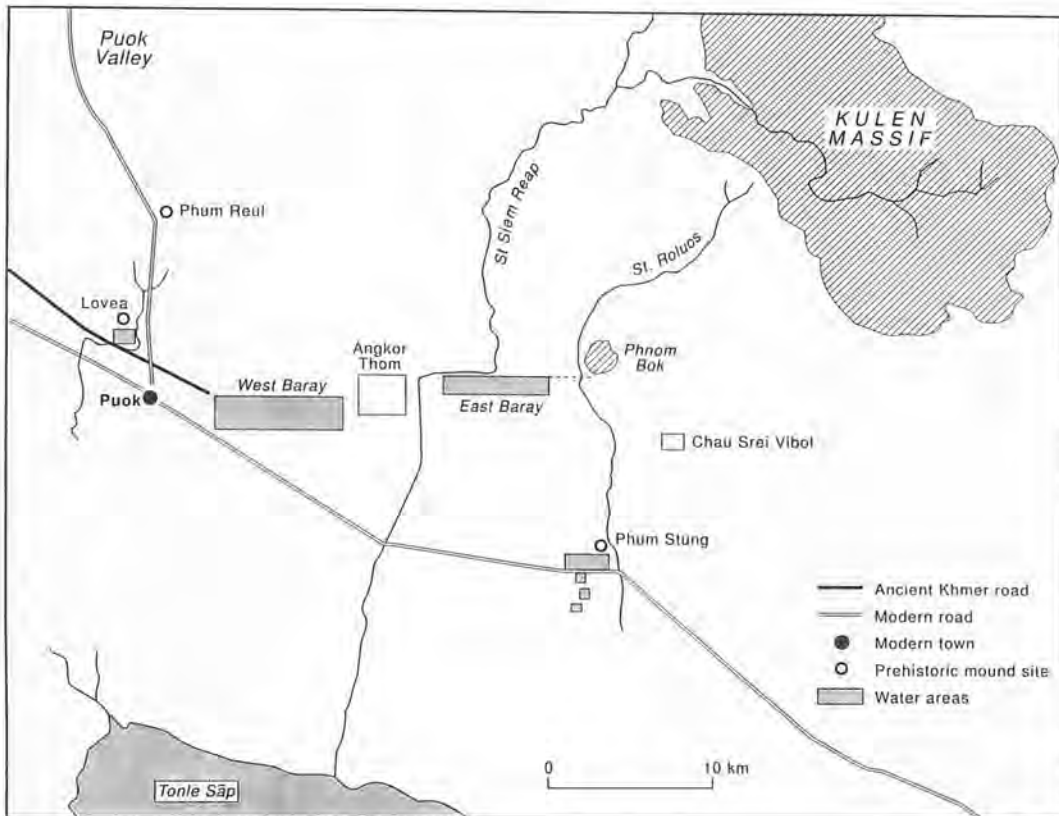
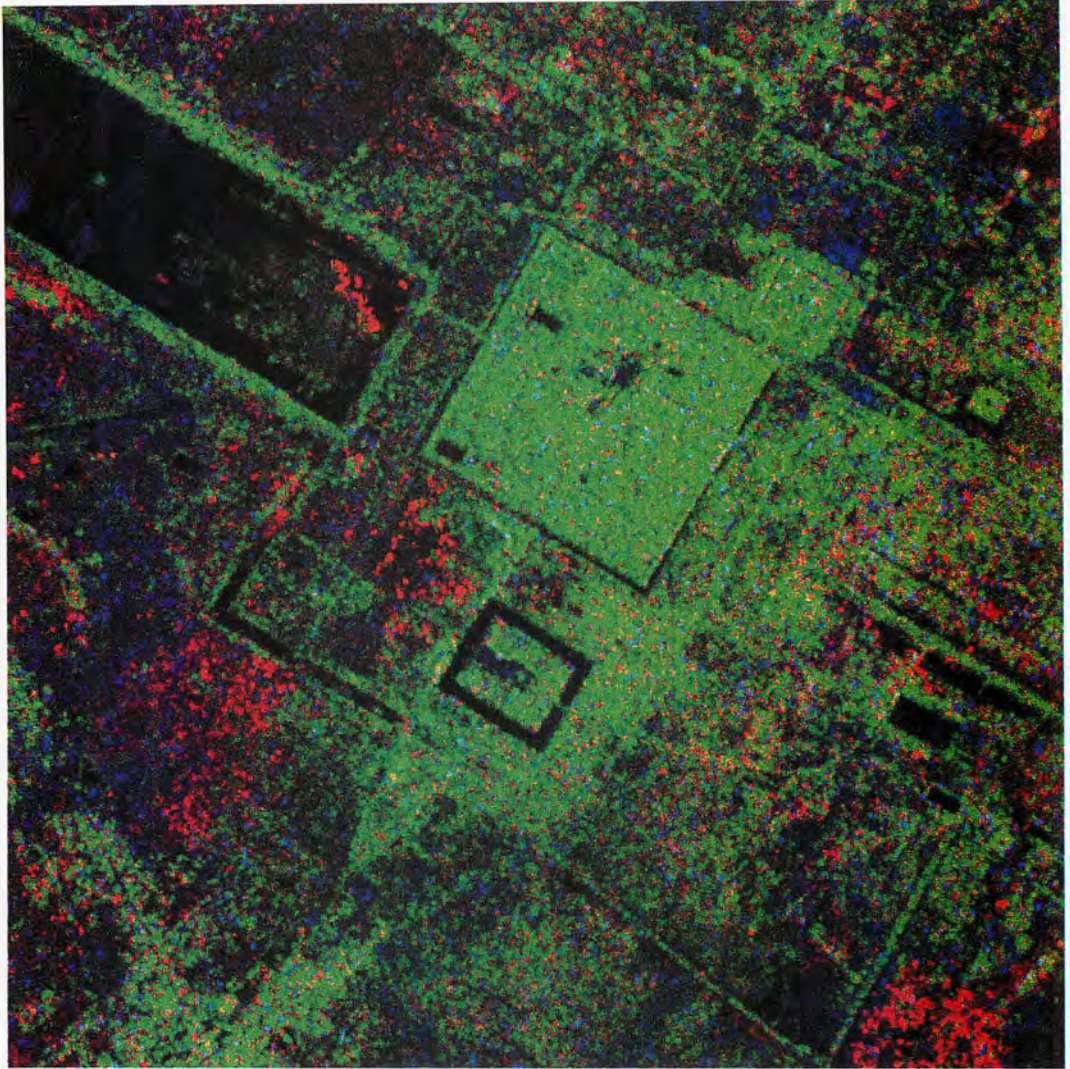


Figure 2. Diagram of Angkor area. The map shows the Puok, Central Angkor, and Hariharalaya sectors discussed in the text.

dar was of an image with data displayed in red, green and blue channels to form a colour composite (Figure 1). The Angkor floodplain may be separated into three sectors from west to east: Puok, Central Angkor and Hariharalaya (Figure 2). The central part of the image has both light and dark areas. The light areas are vegetated, which gives a high or 'bright' radar return. These contrast with black rectangles, water tanks, where the radar signal has diffusely scattered off a smooth surface, giving a low or 'dark' radar return. Other rectilinear features, either water control devices or temple enclosures, are also visible on the image.

Further study of the radar data from Angkor included examination of images produced from the many possible polarization representations of the data. It seemed pertinent to attempt to link scattering mechanisms to man-made and natural features at

Angkor. However, developmental generalizations were questionable given the large number of input parameters: man-made archaeological features such as prehistoric mounds, *barays*, linear dikes, roads, temple *enceintes*; natural elements (rivers, streams, forest); and agricultural land like rice paddy, a range of other crops and forest fellings. The available literature which offer explanations of particular polarimetric signatures are mathematically based, sometimes yielding combinations of three scattering matrices. These, however, are difficult to relate to physical scattering models, and in turn to the landscape of Angkor. Polarimetric radar data has received much attention in recent literature, with discussion of its classification, decomposition and modelling. However, many models of polarimetric radar backscatter have a larger number of terrain input parameters than the radar



**Figure 3.** Scattering mechanism image of central Angkor at L-Band.



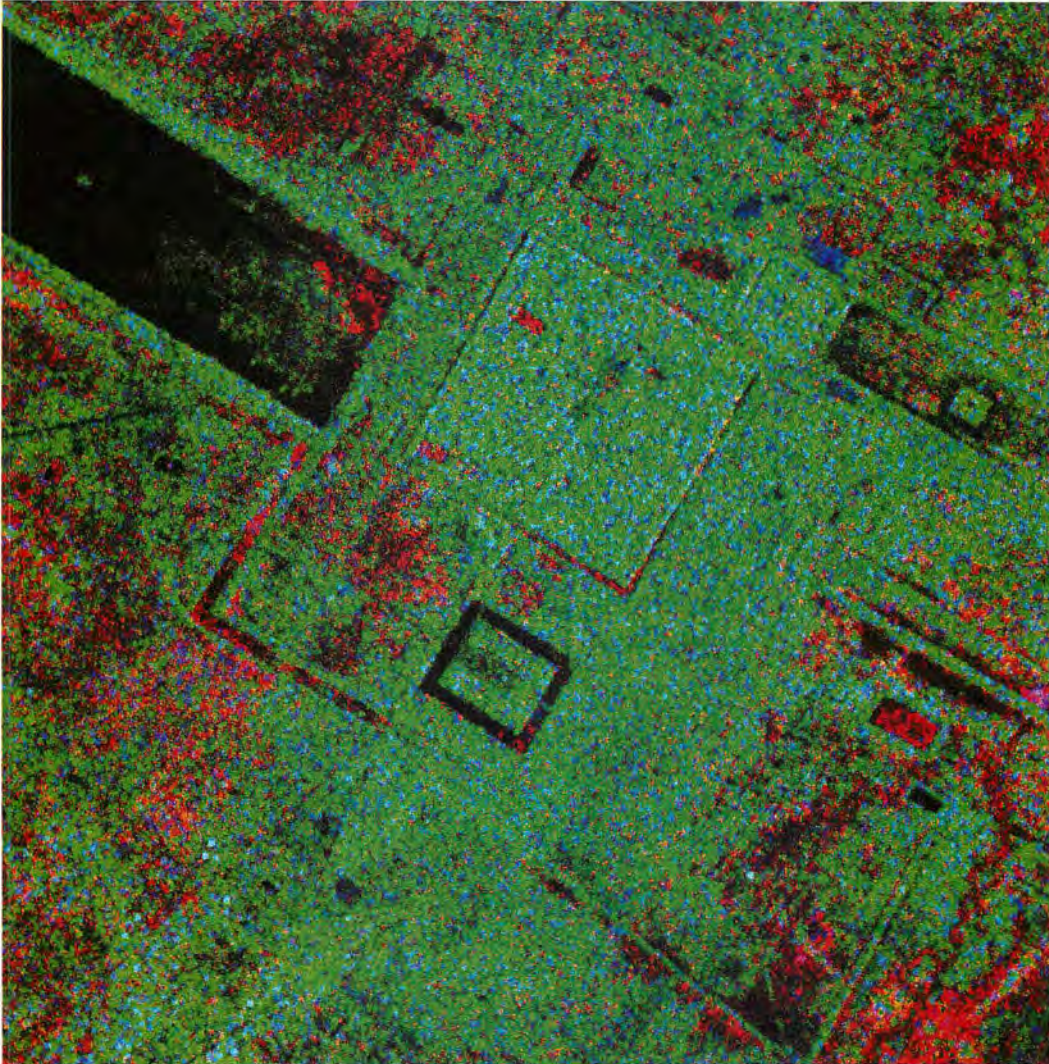


**Figure 4.** Scattering mechanism image of central Angkor at C-Band. Referring to Figure 2, two tanks within Angkor Thom appear black at L-Band but are red at C-Band. The double-bounce, displayed in the red channel, is greater at C-Band than at L-Band. This suggests low-growing vegetation in an inundated area. Low-growing vegetation is also seen in the northeastern corner of the West Baray. Data courtesy of NASA/JPL.



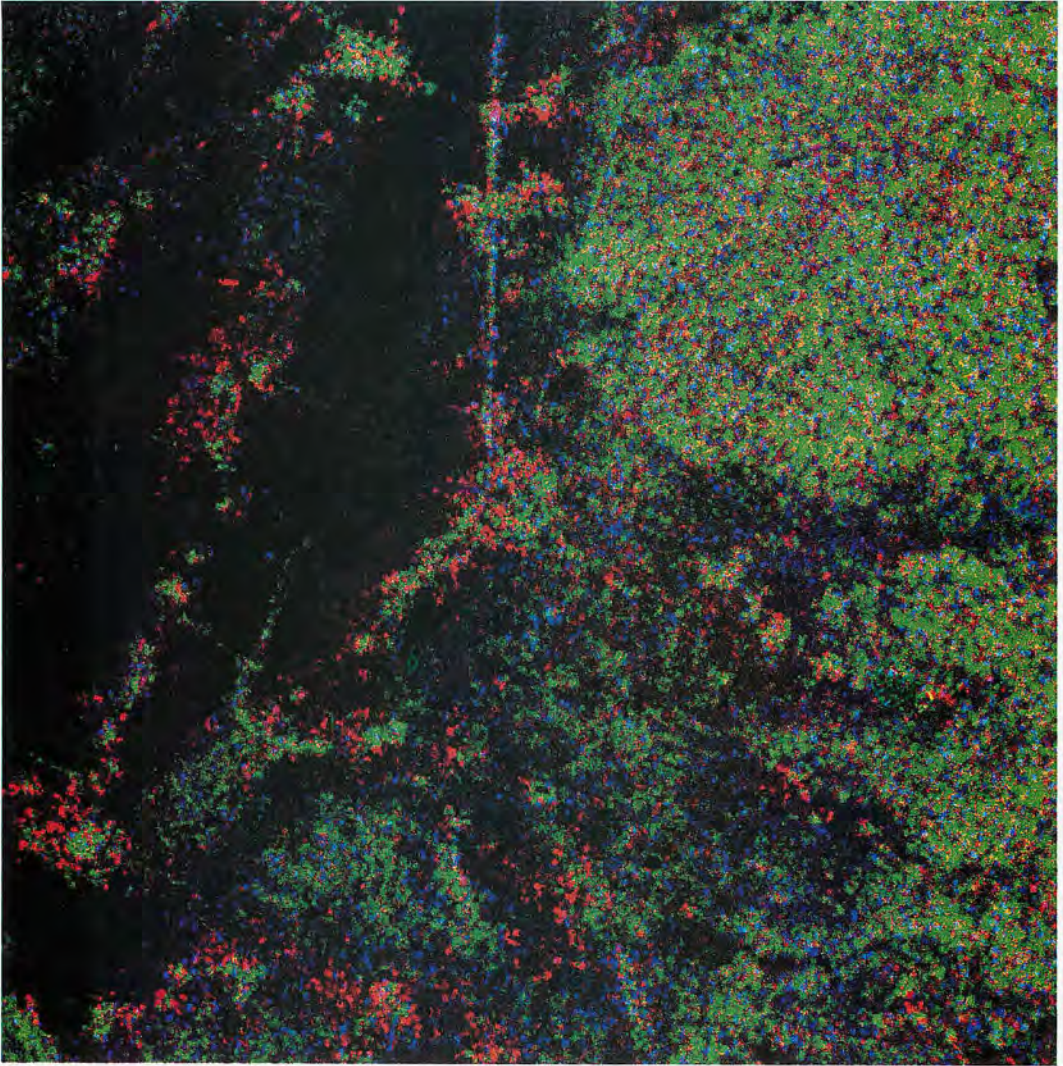
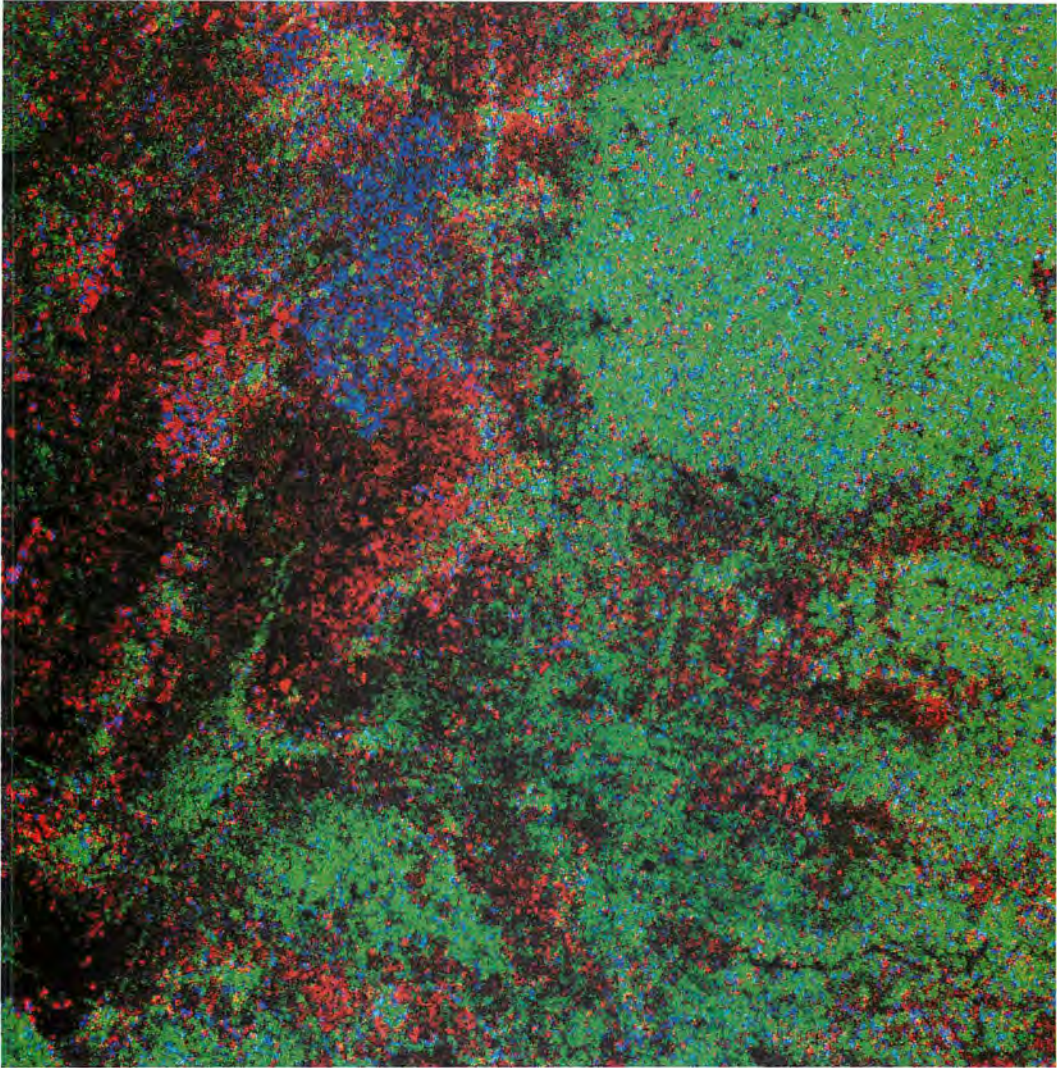


Figure 5. L-Band scattering model image of Lovea-Phum Reul area.





**Figure 6.** C-Band scattering model image of Lovea-Phum Reul area. The U-shaped dike midway between Lovea and Phum Reul is visible on both C-Band and L-Band images. The circular mound of Phum Reul is on the northeast of the larger circle of canopy return seen at L-Band and at C-Band. This larger circle is seen on the bend of the modern road, marked on Figure 2. To the west of the road, the terrain appears black at L-Band, but in the C-Band scattering model shows various types of land-cover, probably a combination of rice field and garden crop cultivation. The bulge of the alluvial fan northeast of the modern road and Phum Reul is defined at both C-Band and L-Band, although the greater penetration of the canopy at the longer L-Band has distinguished both bare (blue) and double-bounce (red) areas within the canopy (green). This is also apparent at C-Band but the shorter wavelength means that the data is predominantly a reflection of the tops of the trees. Data courtesy of NASA/JPL.

measurement output parameters. For example in a forested area inputs might include trunk dielectric constants, ground roughness and dielectric constant, branch size and angular distribution, measurements of tree heights and diameters, and tree density. Complex models have therefore been developed which incorporate large numbers of variables. These models are predictive, capable of solving a 'forward' search for polarimetric signatures assigned to variables in a given area. However, it is difficult, if not impossible, to invert these models to provide initial interpretation and identification of signatures. This dilemma, seen at Angkor, has been a major problem in analyzing the radar data.

### Scattering mechanism model

The model used in this paper classifies polarimetric radar observations in relation to three scattering mechanisms, the behaviour of the radar signal when it hits the terrain. (Freeman and Durden 1992; Norikane and Freeman 1993.) These are double-bounce scatter from a pair of orthogonal surfaces with different dielectric constants, volume or canopy scatter from a cloud of randomly oriented dipoles, and Bragg, odd or surface scatter from a moderately rough surface. In the L-Band and C-Band images generated using this model these mechanisms were displayed in the red, green and blue channels respectively (Figures 3 and 4). While the model has had various applications, it has not been applied in Southeast Asia, and not in relation to archaeological investigation of the terrain.

Previous applications of the model have included a tropical rain forest in Belize; a boreal forest site in Alaska; an arid semi-desert site in Wyoming. The most relevant of these to Angkor is the Belize study, where a land-cover classification was derived for an area measuring 12.3 x 12.6 km. The results of the study showed that the model could be used to the first order to determine the dominant scattering mechanisms for observed backscatter in polarimetric radar

data. This in turn allowed assessment of the fit of the model for the different land-cover types to the surface, volume and double-bounce components. These proved useful in differentiating between different surface cover types, as well as monitoring changes in surface cover.

The same potential is seen in applying the model to Angkor where classification of land-cover is fundamental in understanding terrain and hydrological preferences for prehistoric and historic settlements and water management structures. Decomposition of the radar signatures or measurements into different scattering mechanisms allows the observer to differentiate between different landforms. For example, *terra firma* in the form of raised dikes and mounds can be separated from areas prone to flooding. Rice paddies can be differentiated from areas overgrown with denser vegetation. Circular 'moats' and linear-form canals can be detected by the effect of water on the radar signature, when present beneath a layer of vegetation or with no vegetation cover.

### Puok-Mokak mounds

In the study of early water management in the region of Angkor, the richest distribution of sites is found to the west of the historical urban area, north of the present town of Puok (Figure 2). These sites extend northward some twenty-five kilometres to Mokak, and beyond. The Puok and Mokak mound sites are located along the limits of an alluvial fan spreading southwest from the Kulen massif. Within what appears to be an ancient river bed forming the Puok-Mokak 'corridor', these slightly raised mounds – now just off the edge of the alluvial fan – were isolated through a combination of processes. These included gradual erosion and downcutting of water along the edge of the alluvial fan (north to south and northeast to southwest), continued deposition of sediment, and aeolian action.

The Puok-Mokak fan is separated in its southern portions by remnant streams flowing northeast-southwest. These diffuse the



margins of the terrace in contrast to the clear perimeter of the northern bulge. This pattern is repeated to the east of the Roluos River, but rotated vertically, so that the more clearly delimited portions are to the south. The temple of Chau Srei Vibol rests on the western edge of one of these. As with the Puok area to the west, this combination of canopy and more inundated drainage areas presents a hospitable zone for prehistoric occupation. One of three dikes containing Angkor period kilns has been reported in this area, southeast of Chau Srei Vibol. It is possible that the Indratataka takes advantage of another of these terrace-river interfaces. However, the later building of the East Baray, as well as the diversion of the Stung Siem Reap, have dramatically altered the hydrology of the Hariharalaya area (Moore 1998).

Isolated patches, today village mounds, are generally located west and south of the main spread of the alluvium. Only one, Lovea, is seen as moated on aerial photographs and SPOT images. On scenes generated from the radar data, other mounds appear moated. These sites benefited from the slope of the land, with pooled water around the perimeter of the mound. Man-made moats in some cases exploited this collection process, acting as diversionary structures during times of inundation.

The southern portion of the Puok valley is of particular interest, as the ancient course of the Stung Siem Reap flowed into this area. Clear evidence of this can be seen on the SIR-C images. There is a roughness in the radar return, with contrasting areas of canopy and smoother, inundated rice fields. The northeast-southwest flow of water here in former times is also demonstrated by the U-shaped dike located midway between the mound sites of Phum Reul and Lovea. Lovea, however, is also – and perhaps more closely – associated with a more homogeneous portion of alluvium to the north (Figures 5 and 6).

## Angkor and Northeast Thailand

All of the eleven sites where curvilinear patterns were studied are circular mounds; some are inhabited; all are rural. Their west-east distribution extends some 30 km, from Phum Reul and Lovea on the west to Phum Stung on the east. The most northerly site, Mokak, is 15 km north of Phum Reul (Figure 2). These circular mounds are comparable to sites in Northeast Thailand. The curvilinear patterns visible on images generated from the radar data are similar in form to moats and earthworks which surround the mounds in Northeast Thailand (Moore 1988, 1989, 1992b). With some exceptions, the moats of the Angkor sites are vestigial, not typically apparent on the ground, nor visible on optical imagery.

As suggested by the inclusion of nine out of eleven sites in this region, the Puok area west of Angkor has proved the richest for the present study. The sites are similar in size to many of the mounds of Northeast Thailand. There, mound size is not linked to number of earthworks: Ban Takhong, Buri Ram province (15.13°N x 103.20°E), is 250 metres in diameter and has three earthworks (Moore 1992a). Multiple earthworks are not, however, generally associated with floodplain sites of Northeast Thailand, and to date it is floodplain sites which have been investigated in the Angkor region. (For a description of the sites, see Note 1.)

### Study of curvilinear patterns: method

Although curvilinear patterns are visible on radar colour composites, picture element points (pixels) were selected from L-Band scattering images to focus on the double-bounce, canopy and odd scattering mechanisms. Points were selected where they formed patterns around the generally higher volume return of the central mound, and tabulated by geographical sector. They were then averaged (see Note 2) to give six measures for each site, expressed in decibels (dB). Table 1 separates volume, odd and double-bounce for the mounds, com-

paring results for the scattering model at C-Band and L-Band. A number of sites have an additional exterior 'ring', or fragmented curves, probably remnant earthworks.

A total of 20 to 28 pixels were measured for each site. In most cases the pattern formed a single row, although there were some parts of the curves that widened to two pixels. Given a resolution of approximately 25 metres per pixel for the data, this width approximated the width of the visible moat at Lovea, and also the average of thirty metres for the moats of Northeast Thai sites (Moore 1988). The variation in the measurements provides a remarkably sensitive indicator for ground verification of moats. Each mound, like those in Northeast Thailand, is unique. Any man-made alterations such as moats utilise the mound contours, available water, and the slope of the terrain.

#### Comparison volume, odd, double-bounce return

The volume return was generally brighter at C-Band than at L-Band, although there was variation in both. The standard deviation for the C-Band volume was less than that for the L-Band volume [+0.91 versus +2.38]. A higher return for C-volume than L-volume may suggest low growing vegetation over moist or inundated areas, which

might explain why the moats are not easily seen during ground survey (Note 3). The odd return was not as consistent, at times being nearly the same, and at others the C-Band or L-Band exceeding the other. The averages for the sites at both bands had the highest standard deviation of the three scattering mechanisms [+4.0 for C-Band and +4.2 for L-Band – see Note 4). As with the volume return, a high or bright reading for the double-bounce at C-Band but not at L-Band may suggest low growing vegetation over moist soil or water (Note 5). In many cases, however, the difference between the two wavelengths for the double-bounce was small.

Interpretation of the results from all eleven moats at the mound sites (Table 1) shows that C-Band volume scatter is relatively high (>-7.5 dB) for all sites. In all cases, the volume scatter exceeds the odd or double-bounce. Taken together, in comparison with data from other tropical sites, these suggest the presence of vegetation in the moats. The nature of this vegetation may be assessed through variations in the L-Band volume scatter, usually indicative of different vegetation, canopy height/density or biomass (Note 6).

The high percentage of volume scatter at both L-Band and C-Band suggests woodland or forest (i.e. dense vegetation cover),

<i>Mound</i>	<i>C-volume</i>	<i>L-volume</i>	<i>C-odd</i>	<i>L-odd</i>	<i>C-double</i>	<i>L-double</i>
Reul	-6.0	-9.9	-16.1	-19.3	-16.6	-17.0
Lovea	-7.0	-14.9	-24.6	23.7	-20.3	-12.8
Trei Nhor	-4.8	-9.8	-11.5	-16.0	-12.3	-11.6
Mokak	-7.5	-16.6	-14.9	-21.7	-11.4	-18.3
Ta Saom	-5.4	-15.4	-17.3	-16.6	-15.3	-10.5
Tonle Sa	-6.6	-15.3	-19.2	-17.0	-15.6	-11.0
Chakrey	-7.0	-13.9	-15.6	-23.7	-11.6	-14.6
Pongro	-7.3	-15.0	-16.4	-23.8	-9.4	-13.8
Nokor Pheas	-5.4	-13.5	-23.5	-14.7	-19.1	-14.5
O Dek	-7.2	-16.6	-17.7	-13.2	-19.9	-18.9
Stung	-6.1	-12.2	-12.8	-13.1	-18.8	-18.1
Mean	-6.4	-13.9	-17.2	-18.4	-15.5	-14.6

**Table 1.** Average return (in decibels) of curvilinear patterns for volume, odd and double-bounce at C-Band and L-Band



with no underlying water, as there is comparatively little double-bounce (Note 7). Overall, this suggests *terra firma*; earthworks, with low vegetation cover and moderate vegetation cover. Some sites have a greater (brighter) L-double than L-volume (-2) and less (darker) L-odd than L-volume or L-double, which due to the high L-double, indicates strongly the presence of water underneath the vegetation canopy (see Note 8).

### Conclusion

Study of curvilinear patterns on images generated from the radar data interpreted as remnants of earlier moats at the Angkor mound sites. Also in some cases, the radar data indicates the presence of *terra firma*, which is likely to take the form of (possible prehistoric) dikes at these sites. These results await verification by field or aerial surveys.

Analysis of the many archaeological features of the Angkor site require a repertoire of techniques which thrive on rather than shy away from the immense quantity of data obtained by the NASA/JPL SIR-C/X-SAR radar instrument (Note 9). At the same time, when faced with the huge volume of data, it is difficult to know which variations will provide the most useful insights. Even when single attribute variations are incorporated into correlations, and those into a matrix of correlations, the variables remain too numerous to provide a simple interpretation of their relationship. Another approach to the data is through modelling, such as the example employed here, which fits three scattering mechanisms to polarimetric radar observations.

The focus is on water management features of the prehistoric landscape where images processed from the SAR data depart unequivocally from optical images. The natural and man-made features at Angkor which are relevant to the ancient city fully exploit the sensitivity of polarimetric SAR radar, not only to moisture but all contributors to the biomass. Many factors contrib-

uted to the present vegetation and hydrology of Angkor: the formation of mounds, diversion of river courses, the siting of temples, moats, dikes, and barays. It has not been possible, however, to generate a developmental or conceptual paradigm to explain fundamental aspects of Angkor such as the conservation and control of water. There is no generally accepted geographical and hydrological history of the city, despite years of excellent scholarship investigating the urban zone and its remains. Yet it is commonly agreed that there exists an intimate relationship between those remains and elements such as vegetation and moisture. In the use of microwave remote sensing to study this relationship, new understanding is brought to the critical transition from village to city through exploitation of water resources to alter the terrain. The succession of royal structures at Angkor are often presented as the height of Khmer culture and innovation. However, in the earlier transition from village to city change was equally if not more radical.

### Acknowledgements

Many people and organizations have made this research possible. In particular I express my gratitude to the Jet Propulsion Laboratory, APSARA [Autorité pour la Protection du Site et L'Aménagement de la Région d'Angkor] (Cambodia), the Royal Angkor Foundation (Budapest), the World Monuments Fund (New York), the School of Oriental and African Studies, and the British Academy.

### Notes

1. Description of mounds:

#### Mokak sites

Mokak (13.39n x 103.42e) appears on aerial photographs to have water management structures on its northeast side, whereas the majority of sites show a stronger indication of water control on the downslope side, the southwest. How-

ever, there is an Angkor period tank, and a clear northeast to southwest flow of water.

Sala Khum Ta Saom (13.39n x 103.41) presents a very circular appearance with a continuous moat and an outer earthwork. An area 500 metres north of Phum Ka Ro Lum also shows traces of a moat. It is one kilometre west of Ta Saom, on the opposite bank of the stream running northeast to southwest.

Phum Tonle Sa (13.38n x 103.43e) and Phum Pongro (2) (13.37n x 103.43e) are four kilometres south east of Mokak. On 1954 French aerial photographs Phum Tonle Sa presents clear evidence of water pooling on the south of the mound. An additional barrage and small tank are located to the northeast. At Pongro, the outer perimeter of a band of rice fields encircling the mound suggests that remnants of an earthwork remain. Phum Romiet, 2.5 kilometres northeast of Phum Pongro, also shows evidence of a moat, but was not included in the data processed for the present study.

Phum Chruoy Chakrey (13.36n x 103.42e) and a site 500 metres north east of Phum Nokor Pheas (13.36n x 103.43e) parallel the main north-south road (Rte. 671) at the same latitude, on the west and east respectively. Nokor Pheas appears to be uninhabited, although 1:50,000 maps do note a temple. It forms a 'bridge' across the south end of a northeast-southwest inundated strip, possibly a former streambed. In this context, it – and all the sites on the Mokak and Puok scenes except Chakrey – conform to the pattern of being slightly isolated from the main spread of alluvium. Chakrey's hydrological relationship is to Mokak and Ta Saom to the north.

#### **Puok sites**

Phum Trei Nhor (13.34n x 103.43e) is 3 kilometres further south along the road. As with Nokor Pheas and Phum Chakrey, there is a parallel site on the west of the road, Phum Thipdei, although it was not included in the present study.

Phum Reul (2) (13.33n x 103.44e) is initially difficult to distinguish on images generated from the radar data. The mound, like that of Trei Nhor, is nestled close to the edge of the alluvium. However, the backscatter from the mound is merged with return from three to four villages to the south and south west of the mound. The most southerly of these may have an inundated area on its southwestern perimeter. Thus what initially seems a contiguous mass is several different areas. Further verification is needed for the diameter of Reul: measured as 200 metres, ground check in December 1996 and April 1997

suggests the mound is larger.

The Lovea mound (13.28n x 103.43e) is recorded as being the largest of the sites with a diameter of 350 metres. Further ground survey, however, may reduce this. For example, the present monastery, east of the site, may not have formed part of the original mound. On the other hand, Lovea remains unique in the visible remnants of two earthworks, which may be a reflection of an importance accorded to its size. Other interesting aspects of the site are the U-shaped bund or dike midway between Phum Reul and Lovea, the canal running north from the site, the east-west dike north of the site, and the large rectangular *baray* to the south.

#### **Hariharalaya sites**

Phum Stung (13.22n x 103.45e). The mound was visited several times, between December 1992 and April 1995. An exterior earthwork is faintly visible at Phum Stung on aerial photographs [most visibly on the 1945 Williams-Hunt Collection, somewhat on the French 1954 1:40,000 cover]. Moat remnants were confirmed on the ground on the east and west sides of the mound. The mound is largely uninhabited, with parts given over to upland crops. A stone tool was recovered from a cornfield, along with a few pottery sherds (Moore 1997).

O Dek (O Spean Dek or Kaek, 13.22n x 103.57e) appears quite clearly on aerial photographs as a mound nestled in a curve of a small stream. Ground survey (not yet possible due to security problems) may confirm a smaller mound diameter than recorded (300 metres).

2. The measurements were taken from files generated by A. Freeman. The data was transformed from a 1-254 scale to decibels with Excel, using the formula:  $10 * \text{LOG}_{10} ((255 - C27) * 0.0039212 + 0.0001)$ . The decibel measurements were then averaged per sector and as a whole.

3. Sites of particular interest to check in this regard would be Ta Saom and O Dek, although they are difficult to access. Lovea, more accessible, could be checked on the southwest sector where the C-volume and L-volume difference was quite high [-6.3 versus -22.4], and then compared to other sectors, such as the southeast or northwest where the difference is less [-6.5 versus -11.7, and -7.7 versus -12.7].

4. Only at Nokor Pheas was the L-odd much brighter than the C-odd [-14.7 versus -23.5]. In comparing the odd and double-bounce return,



many C-Band returns were similar. Pongro was an exception with a double-bounce return of -9.4 but only -18.4 for the C-Band odd. This was the case for all four sectors of Pongro, although the difference was the greatest in the southwest sector [-13.6 versus -4.7].

5. This was the case at Mokak, where a bright C-return and dark L-return were seen on average for all three scattering mechanisms. At Ta Saom the L-Band return was less [-15.3] than the C-Band [-10.5]. At Tonle Sa the double-bounce was -15.6 at C-Band and -11.0 at L-Band. But at Lovea, the L-Band was much brighter than the C-Band [-12.8 versus -20.3]. Recalling the much brighter C-Band return for volume in the southwest sector of Lovea, it is of note that the double-bounce difference was primarily generated by the data from the southwest sector: the C-Band return was only -27.6 while the L-Band was -8.3. Mokak and Pongro provided the most consistency, with all or nearly all sectors having brighter C-Band than L-Band returns for volume and double-bounce.

6. The moat at Phum Reul, for example, has:

C-volume = -6.0 dB	L-volume = -9.9 dB
C-double = -16.6 dB	L-double = -19.3 dB
C-odd = -16.1 dB	L-odd = -17.0 dB

7. When Phum Reul is compared to the other moats by comparing the relative levels of double-bounce, volume and odd-bounce scattering in each frequency band it can be seen that the sites vary. For example, Phum Trei Nhor has:

C-volume = -4.8 dB	L-volume = -9.8 dB
C-double = -12.3 dB	L-double = -11.6 dB
C-odd = -11.5 dB	L-odd = -16.0 dB

These figures indicate, relative to Phum Reul, that Trei Nhor has a greater amount of dense vegetation over water in the moat. Both O Dek and Phum Stung, have a relatively high L-odd (~-13 dB) and low L-volume (-16.6 dB) and moderate L-volume (-12.2 dB) respectively.

8. This is seen at Lovea, Trei Nhor, Mokak, Ta Saom, Tonle Sa, Chakrey, and Pongro. Of all the sites, based on L-volume scatter, Phum Reul and Trei Nhor have the highest levels of vegetation relative to the other sites. The figures from Nokor Pheas suggest a moderate level of vegetation and perhaps a mixture of *terra firma* and inundated vegetation.

9. Further data on the sites was acquired on 6

December 1996, as part of the NASA/JPL Pacific Rim Campaign. The AIRSAR equipment included P-band (68 cm) in addition to C-band and L-band, and the ability to process data in polarimetric (POL SAR) and topometric (TOP SAR) modes.

## References

- Freeman, A. and Durden, S. 1992. A three-component scattering model to describe polarimetric SAR Data. *SPIE* 1748, Radar Polarimetry: 213-24.
- Norikane, L. and Freeman, A. 1993. *User's Guide to MacSigma*.
- Moore, E. H. 1988. *Moated Sites in Early North East Thailand*. Oxford: BAR International Series 400.
- Moore, E. H. 1989. Water management in Early Cambodia: Evidence from Aerial Photography. *The Geographical Journal* 155 (2): 204-14.
- Moore, E. H. 1992a. Water-enclosed Sites: links between Ban Takhong, Northeast Thailand, and Cambodia. In Rigg, J.(ed.) *The Gift of Water, Water Management, Cosmology and the State in South East Asia*, pp. 26-46. SOAS: University of London.
- Moore, E. H. 1992b. Moated settlement in the Mun Basin. In Glover, I. & E. (eds) *Southeast Asian Archaeology 1986*, pp.210-22. Oxford: BAR International Series, 361.
- Moore, E. H. 1997. The prehistoric habitation of Angkor. In Manguin, P.-Y. (ed.), *Southeast Asian Archaeology 1994*, Vol. 1. Hull: Centre for South-East Asian Studies, pp. 27-36.
- Moore, E. H. 1998. The East Baray: Khmer water management at Angkor. *Journal of Southeast Asian Architecture*, University of Singapore, (Forthcoming)

KEYWORDS – CAMBODIA, ANGKOR, SATELLITE IMAGING, RADAR, KHMER, SPATIAL ANALYSIS

